Journal of Solid State Chemistry 181 (2008) 2442–2447

Contents lists available at ScienceDirect

Journal of Solid State Chemistry

journal homepage: www.elsevier.com/locate/jssc

Consolidated silica glass from nanoparticles

Thomas G. Mayerhöfer [a,d,*], Zhijian Shen [b], Ekaterina Leonova [c], Mattias Edén [c], Antje Kriltz [a], Jürgen Popp [a,d]

[a] Institut für Physikalische Chemie, Friedrich-Schiller-Universität, Lessingstraße 10, D-07743 Jena, Germany
[b] Division of Inorganic Chemistry, Arrhenius Laboratory, Stockholm University, S-106 91 Stockholm, Sweden
[c] Division of Physical Chemistry, Arrhenius Laboratory, Stockholm University, S-106 91 Stockholm, Sweden
[d] Institut für Physikalische Hochtechnologie e.V., Albert-Einstein-Str. 9, D-07745 Jena, Germany

ARTICLE INFO

Article history:
Received 29 January 2008
Received in revised form
16 May 2008
Accepted 7 June 2008
Available online 11 June 2008

Keywords:
Glass
Spark Plasma Sintering
Ellipsometry
TEM
Infrared spectroscopy
Raman spectroscopy
UV–Vis–NIR spectroscopy
NMR spectroscopy

ABSTRACT

A dense silica glass was prepared by consolidating a highly dispersed silicic acid powder (particle size <10 nm) with the Spark Plasma Sintering (SPS) technique. The glass was characterized by ellipsometry, transmission electron microscopy (TEM), infrared reflectance and transmittance spectroscopy, as well as by Raman, UV–Vis–NIR and solid-state nuclear magnetic resonance (NMR) spectroscopy. The prototypic sample showed a transmittance of about 63% compared to silica glass in the UV–Vis spectral range. Based on the results of infrared transmittance spectroscopy this lower transparency is due to the comparably high water content, which is about 40 times higher than that in silica glass. ^{1}H magic-angle spinning (MAS) NMR confirmed an increase in hydroxyl groups in the sample prepared by SPS relative to that of the conventional SiO_2 reference glass. Aside from the comparably high water content, we conclude from the similarity of the IR-reflectance and the ^{29}Si MAS NMR spectra of the SPS sample and the corresponding spectra of the conventionally prepared silica glass, that the short- and medium-range order is virtually the same in both materials. Raman spectroscopy, however, suggests that the number of three- and four-membered rings is significantly smaller in the SPS sample compared to the conventionally prepared sample. Based on these results we conclude that it is possible to prepare glasses by compacting amorphous powders by the SPS process. The SPS process may therefore enable the preparation of glasses with compositions inaccessible by conventional methods.

1. Introduction

Spark Plasma Sintering (SPS) employs a combination of a pulsed direct current and uniaxial exerted pressure to compact powders. Its main advantage compared to conventional techniques like, e.g., hot pressing, is that it allows the powders to be consolidated at comparably low temperatures in a very fast manner, thus suppressing the growth of particles completely or at least for the most part. In addition, in most cases, the compacted samples reach nearly (99%+) the theoretical density [1–4].

SPS has been used to prepare a wide spectrum of ceramic materials, including biomaterials [5,6], composites [7,8], dielectrics [9,10], superconductors [11,12] and transparent ceramics [13,14]. Glassy materials have also been prepared. However, to our knowledge, these glasses all belong to the family of metallic glasses (e.g., Refs. [15–17]). In this paper, we report the successful use of the SPS process for the compaction of highly dispersed silicic acid leading to SiO_2 glass and the structural characterization of the compacted samples. Our intention is not to promote a replacement of well-established methods to fabricate glassy SiO_2 like, e.g., flame hydrolysis or plasma-activated chemical vapor deposition (PCVD) [18]. Rather, the compaction of SiO_2 by SPS may be viewed as a proof of concept, possibly enabling the fabrication of glasses outside the compositional range of conventional preparation methods, i.e. the classical melting followed by fast cooling. In this classical way of glass preparation phase-separation or crystallization can be suppressed only for certain ranges of composition. Segregation processes need time, so we assume, that the fast SPS process will be able to broaden the range of glass formation. Possible targets are, e.g. pure TiO_2 glass, barium titanate glasses without dopants of classical network formers or phosphate-titanate glasses in a wider range of composition, e.g. for photonic applications.

In this field of application, the SPS process has already proven to permit the compaction of nano-sized ceramic powders, thus enabling the preparation of transparent ceramics [13,14]. Yet, the transparency of such materials is comparably low either due to absorption or a non-complete suppression of light scattering or a combination of both. The effect of light scattering is especially

* Corresponding author at: Institute of Photonic Technology, Albert-Einstein-Str. 9, Jena, Germany. Fax: +49 3641 206 399.
E-mail address: Thomas.Mayerhoefer@uni-jena.de (T.G. Mayerhöfer).

0022-4596/$ - see front matter © 2008 Elsevier Inc. All rights reserved.
doi:10.1016/j.jssc.2008.06.011

obvious from the typical drastic decrease of transmission with decreasing wavelengths. Such a decrease of transmission is completely absent in the SPS-compacted SiO_2 in contrast to transparent ceramics [13], where scattering cannot be avoided, as will be shown in the beginning of Section 3.

2. Experimental details

2.1. Preparation of the samples

2.1.1. SiO_2 glass (reference sample)

As reference sample we choose commercially available SiO_2 glass, purchased from JENAer Glaswerk. The reference sample was prepared by melting a Brazilian rock crystal using an oxyhydrogen burner based on a method developed by the company Heraeus in 1899.

2.1.2. SPS sample

The precursor used in this work is an amorphous SiO_2 powder (HDK T40, Wacker Chemie AG). The particle size of the powder is less than 10 nm according to transmission electron microscopy (TEM) measurements. The samples were consolidated in vacuum in an SPS apparatus, Dr. Sinter 2050 (Sumitomo Coal Mining Co. Ltd., Japan). The powder precursor was loaded in cylindrical carbon dies with an inner diameter of 12 mm. The samples were heated via a pulsed DC current that passes through the pressure die, i.e. the pressure die also acts as a heat source. A pulse duration of 3.3 ms and a sequence consisting of 12 pulses followed by two periods (6.6 ms) of zero current were used. The temperature was automatically raised to 600 °C within 3 min, and from this point and onwards it was monitored and regulated by an optical pyrometer focused on the surface of the die. Systematic sintering experiments (cf. Fig. 1) were carried out with the aim of determining the minimum temperature, 1000 °C, required to fabricate fully densified samples. This temperature was chosen as the maximum temperature for the SPS process and was held for 5 min, while a uniaxial pressure of 100 MPa was exerted on the sample. After the SPS process the sample was annealed at 900 °C for 5 h in air in order to remove surface graphite. Additionally, a partially consolidated sample was prepared for the TEM measurements at a maximum temperature of 900 °C, held for 1 min, while exerting a pressure of 100 MPa. No further treatment was carried out on this sample.

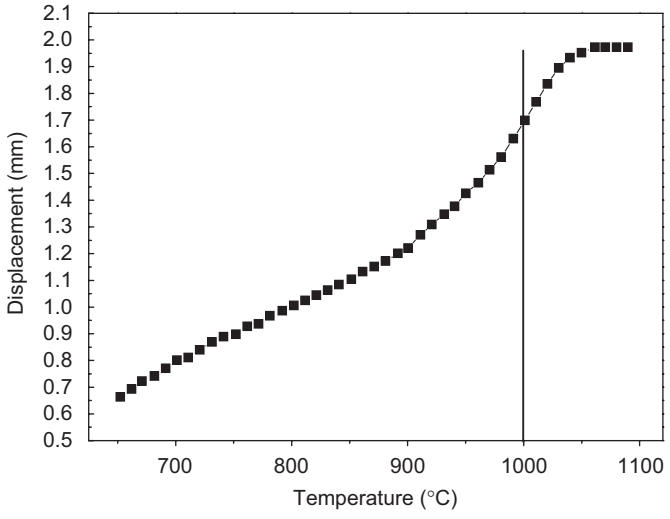

Fig. 1. Real-time shrinkage recorded during the SPS process plotted versus temperature. The experiment was carried out under a constant uniaxial pressure of 50 MPa with a constant heating rate of 100 °C/min above 650 °C. Maximum densification rate is achieved above 1000 °C.

2.2. Characterization methods

2.2.1. Infrared spectroscopy

Infrared spectra were recorded using a Bruker IFS 66 in the mid-infrared (400–6000 cm^{-1}) and in the far-infrared spectral range (100–450 cm^{-1}) with a spectral resolution of 2 cm^{-1} (1 cm^{-1} interpolated) in transmittance and reflectance mode. The transmission spectra were normalized to a sample thickness of 1 mm. For the reflection measurements an accessory from Zeiss™ was employed, which operates at a (fixed) angle of incidence of 20°. Due to the non-near normal incidence we used KRS-5 (MIR) and a PE-wire grid polarizer (FIR) to generate perpendicular to the incidence plane polarized light. Reference measurements were carried out on a gold mirror. The area of inspection was limited by a circular aperture with a diameter of 5 mm.

2.2.2. Raman spectroscopy

Raman measurements were carried out with a Jobin-Yvon T64000 micro-Raman-spectrometer with an attached Olympus microscope using the 514.5 nm radiation line of an Ar–Kr gas laser. A second series of measurements was performed with a HR800 micro-Raman-spectrometer (Horiba/Jobin Yvon) equipped with a 2400-groove mm^{-1} grating and a cryogenically cooled charge-coupled device (CCD) detector employing the 244 nm line of a frequency-doubled Ar-ion laser.

2.2.3. UV–Vis–NIR spectroscopy

The UV–Vis–NIR spectroscopic measurements were carried out with a Specord S100 diode array spectrometer (Zeiss) in absorption mode at plan-parallel polished samples. The integration time was 25 ms and the number of scans per spectrum 1000. The spectra were recorded from 190 to 1020 nm with a resolution of 0.8 nm. As reference we used air. The spectra were smoothed by an 11-point Savitsky–Golay function. As in the infrared, the transmission spectra were normalized to a sample thickness of 1 mm.

2.2.4. TEM measurements

The partially consolidated sample was checked by TEM (JEOL JEM-3010). As revealed in Fig. 2, the presence of voids in this sample is obvious and the initial particles have a diameter of about 10 nm.

2.2.5. Solid-state NMR spectroscopy

Magic-angle spinning (MAS) nuclear magnetic resonance (NMR) data were collected at 9.4 T using a Varian/Chemagnetics Infinity-400 spectrometer, giving Larmor frequencies of −400.2 and 79.5 MHz for ^{1}H and ^{29}Si, respectively. Approximately 320 mg of finely ground samples were filled in 6 mm zirconia rotors and spun at the MAS rates 8.00 and 8.50 kHz for ^{29}Si and ^{1}H acquisitions, respectively. For each observed nucleus, the experimental conditions were identical for the two samples. ^{29}Si acquisitions employed 35° pulses with 50 min relaxation delays and additional equilibration periods of 5 h inserted prior to the start of data collection, as well as after completing the first half of the total number of 96 signal transients/sample. Each ^{1}H spectrum was recorded by starting each of the 64 co-added signal transients by a comb of saturation pulses, followed by a relaxation delay of 420 s and a 90° read pulse. The ^{1}H longitudinal relaxation times (T_1) were found to be relatively long and dependent on the overall ^{1}H content in each sample; we estimated $T_1 \sim 190$ s and ~ 65 s for the reference silica glass and the SPS sample,

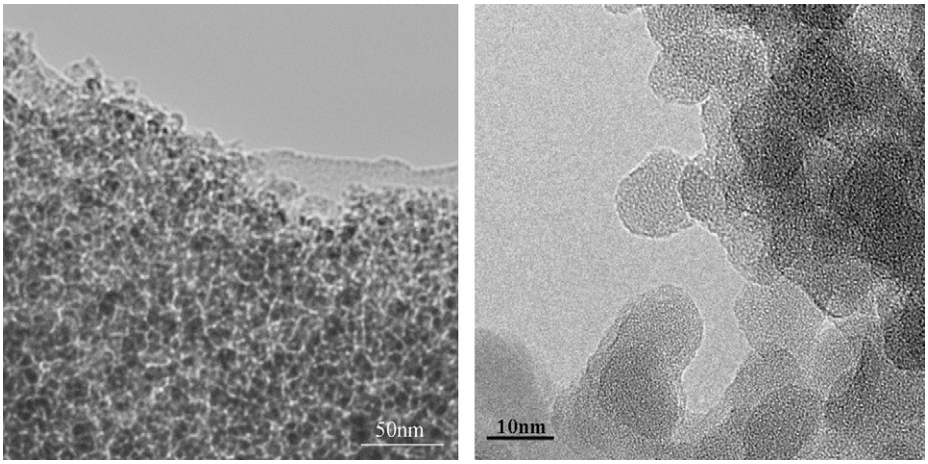

Fig. 2. TEM images of a partially consolidated sample prepared at 900 °C for 1 min under a uniaxial pressure of 100 MPa, revealing the size of the initial particles and the voids present.

respectively. ^{29}Si and ^{1}H chemical shifts (deshielding units) are quoted relative to tetramethylsilane (TMS).

2.2.6. Ellipsometric measurements

To determine the refractive index *n* and absorption index *k*, variable angle spectroscopic ellipsometry (VASE) measurements were carried out with a SE400 ellipsometer (Sentech) using the wavelengths 401.0 and 632.8 nm. The angle of incidence was varied from 40° to 85° performing a measurement every 5°. The reference sample had been covered at the backside with carbon black prior to the measurement to avoid backside reflection. To transform the results of the measurements into values of *n* and *k*, we modeled them assuming a layered system consisting of a Cauchy-SiO_2 substrate and air.

2.2.7. Thermogravimetric analysis

The thermogravimetric study was performed in a Setaram TAG 24 unit in the temperature interval 20–900 °C using a heating rate of 10 K/min. The Spark Plasma Sintered compact was crushed into powder and 12 mg of this powder was loaded into an Al_2O_3 cup. The experiment was performed in oxygen.

3. Results and discussion

Fig. 3 shows the transmission spectrum of the SPS-compacted highly dispersed silicic acid (HDSA) in comparison with that of a conventionally prepared silica glass. Similar to conventionally prepared silica glass, the SPS sample shows a transmission, which is nearly constant between 200 and 1000 nm. Unlike to the latter, however, which possesses a transmission of about 99% in the investigated spectral range, the transmission of the former reaches only about 63%. Compared to transparent ceramics, e.g. SPS-compacted nanocrystalline MgO, this is still impressive, since these ceramics attain such values only in the NIR spectral range and show a strong decrease of the transmission in the visible range due to scattering [13]. Since the transmission is nearly constant in the SPS-compacted HDSA, scattering can be excluded as a reason for the lower transmittance compared to conventionally prepared silica glass. The loss of light intensity must therefore stem from absorptive processes, which must have their origins in the structure of the material.

One possibility to probe the structure of the SPS-compacted HDSA is infrared spectroscopy. In the case of glasses, IR-reflectance spectroscopy is usually applied, since the dipole moment changes associated with the IR-active vibrations of the

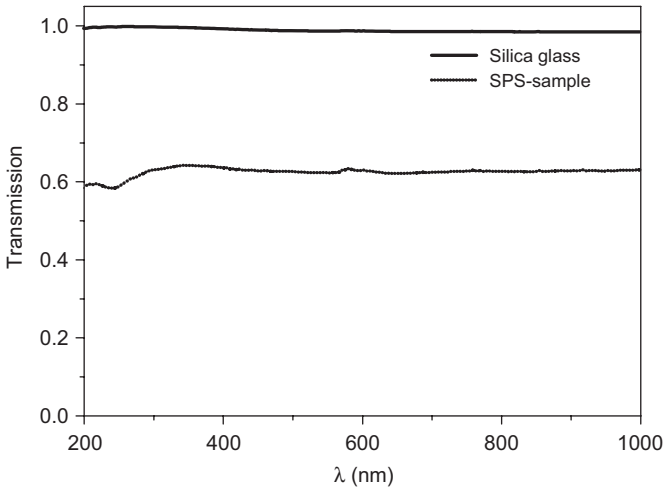

Fig. 3. Transmittance of the compacted highly dispersed silicic aid powder in the UV–Vis–NIR-spectral region compared to that of a conventionally prepared silica glass (normalized to a sample thickness of 1 mm).

SiO_4 tetrahedron are too strong to allow for a registration of transmitted radiation below about 2000 cm^{-1}, except for samples thinner than approximately 10 μm. Since, on the other hand, the bands above 2000 cm^{-1} are too weak to appear in the reflectance spectrum, only the spectral range between 200 and 1900 cm^{-1} is displayed in Fig. 4, which compares the spectrum of the SPS-compacted HDSA with that of the conventionally prepared sample. The peak at 1123 cm^{-1} in the spectra is attributed to the asymmetric Si–O–Si stretching vibration (AS). The shoulder at 1220 cm^{-1} is usually accepted as being caused by the longitudinal optical phonon of the same vibration [19,20]. An alternative interpretation would be that both features are due to transversal optical excitations of two different AS modes called AS_1 and AS_2 [21–24]. The absence of peaks around 970 and 3430 cm^{-1}, which would indicate the presence of Si–OH moieties [24,25], e.g. as present in HDSA, suggests that the water bound at the surface of the starting material has mostly been removed. The comparably weak peak around 785 cm^{-1} is due to the symmetric Si–O–Si stretching vibration and the strong band around 480 cm^{-1} is attributed to the Si–O–Si bending vibration [21–24]. Aside from the lower intensity of the reflectance from the SPS-compacted HDSA, both spectra show an overall agreement with regard to peak positions, peak shapes and relative intensities. This agreement suggests that the structure of both samples is widely similar,

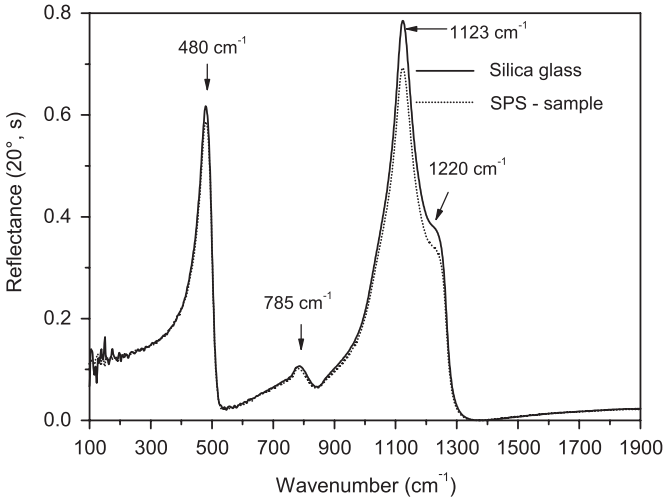

Fig. 4. Reflectance spectra of the SPS sample and the conventionally prepared silica glass (perpendicular polarized incident light, angle of incidence 20°).

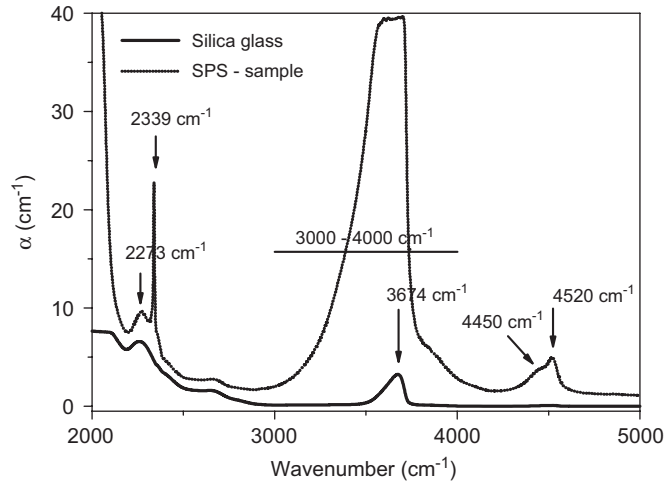

Fig. 5. IR-absorption spectra of the SPS sample and the conventionally prepared silica glass in the range between 2000 and 5000 cm^{-1}.

at least in the surface and the near-surface regions probed by IR-reflectance spectroscopy. A discrepancy between the samples, however, is revealed upon comparison of the IR-absorption spectra shown in Fig. 5, which expose a 40 times higher water content of the SPS sample compared with the conventionally prepared silica glass. This information can be extracted by comparing the area of the broad bands located at 4450 and 4520 cm^{-1}. These bands are attributed to the combinations $\nu_{SiO-H}+\nu_{Si-OH}$ and $\nu_{SiO-H}+\nu_{as,Si-O-Si}$, with the ν_{SiO-H} being located around 3674 cm^{-1}. Unfortunately, it is not possible to evaluate if there is any free water present in the SPS sample, since the range around 1595 cm^{-1}, wherein the deformation vibration of the water molecule is excited, is not utilizable. The presence of free water molecules is improbable considering the nature of the SPS process. In addition to the aforementioned peaks, we find a peak at 2273 cm^{-1}, which is present in the spectra of both samples, and an additional sharp peak at 2339 cm^{-1}, which cannot be found in the spectrum of the conventionally prepared sample. The former peak is probably the second harmonic of the asymmetric Si–O–Si stretching vibration, even if it is displaced to higher wavenumbers compared to $2\nu_{as,Si-O-Si}$ (TO). The shift may be explicable by a merging of the TO- and the LO-second harmonic. The latter peak at 2339 cm^{-1} is possibly an indication of Si–H bands. Its sharpness

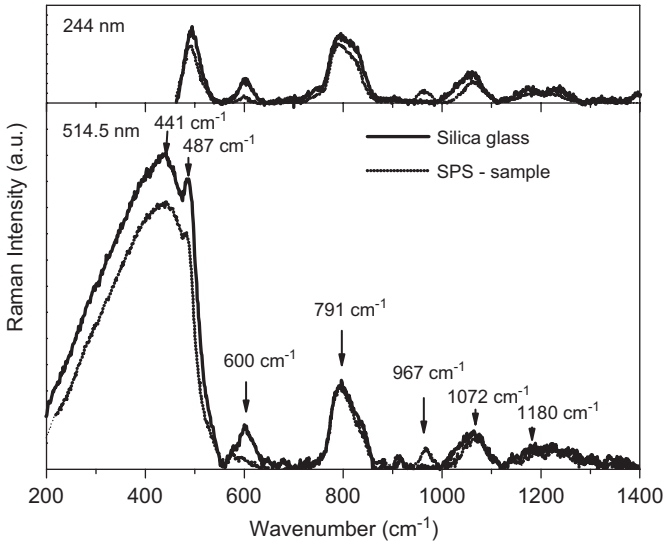

Fig. 6. Raman spectra of the SPS sample and the conventionally prepared silica glass in the range between 200 and 1400 cm^{-1} (244 nm excitation wavelength: 450 and 1400 cm^{-1})

is unparalleled and somewhat puzzling; therefore this assignment should be seen as being tentative.

The Raman spectra (Fig. 6) seem to be more sensitive to structural changes compared to the IR-reflectance spectra. Besides the bands, which have counterparts in the IR spectra (441 cm^{-1} $\delta_{Si-O-Si}$, 791 cm^{-1} $\nu_{as,Si-O-Si}$, 1072 cm^{-1} $\nu_{as,Si-O-Si}$ (TO), 1180 cm^{-1} $\nu_{as,Si-O-Si}$ (LO)), we find three bands, which do not occur in the IR-reflectance spectra. The first can be found at 967 cm^{-1} and is assigned to ν_{Si-OH}. The other two bands at 487 and 600 cm^{-1} are being discussed very controversial in the literature. First, they were seen as "defect bands", since their intensity increased with neutron irradiation [26]. Nowadays they are usually attributed to vibrations of three- (600 cm^{-1}) and four-membered rings (487 cm^{-1}). Interestingly, these bands have lower intensities in case of the SPS sample. This may be a consequence of the stronger presence of OH groups in this sample, but it might also be, that the formation of such rings is hindered by the SPS process.

From the high-wavenumber range of the reflectance spectra it could already be concluded that the refractive indices in the visible of the silica glass as well as of the SPS-compacted sample must be quite similar. This conclusion is proved by the results of the VASE measurements. These results were first fitted assuming a layered system consisting of air/Cauchy-SiO_2 substrate/air. This fit yielded a good match only in the case of the silica glass. For the SPS-compacted sample it was necessary to assume an additional very thin layer of amorphous carbon at the substrate surface to obtain a satisfying match between model and the experimental results. Carbon was chosen because of the possibility of a transfer of carbon into the sample during the preparation [27]. However, the assumption of a carbon surface layer is unlikely, since such a layer would have been removed during the polishing of the sample surface. More probable is that amorphous carbon permeated into the SiO_2 and formed a layer consisting of inclusions of amorphous carbon surrounded by a SiO_2 matrix. Unfortunately, this more sophisticated model could not be applied due to limitations of the software used for the analysis of the VASE data.

The parameters employed for the fit of the VASE data are summarized in Table 1. The refractive index was modeled by the following Cauchy equation:

$$n(\lambda) = n_0 + 10^2 \frac{n_1}{\lambda^2} + 10^7 \frac{n_2}{\lambda^4}, \quad [\lambda] = nm. \tag{1}$$

Table 1
Results of VASE

Sample	n_0	n_1	n_2	k	Thickness (nm) (amorphous C)
Silica glass	1.463	−47.2	114.8	0.000	–
SPS sample	1.463	−18.3	56.4	0.000	1.80

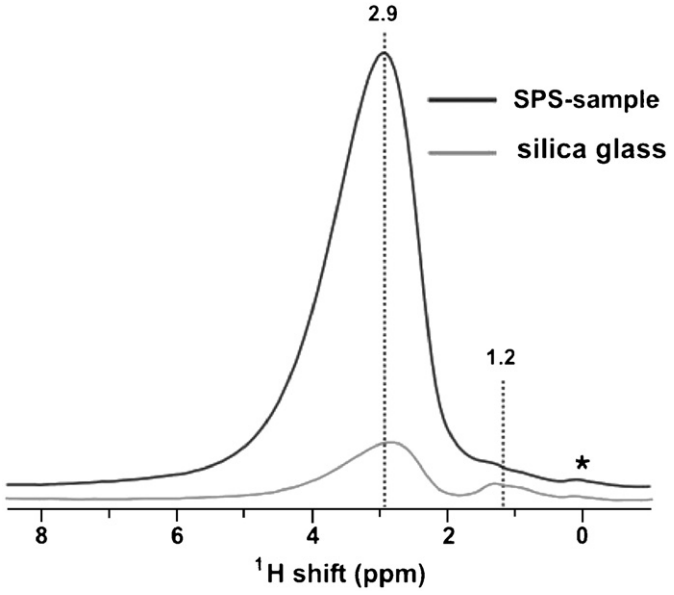

Fig. 7. ^{1}H MAS NMR spectra of SiO_2 glasses prepared using SPS (top) and by a conventional technique (bottom). Their only essential difference is the intensified signal around 2.9 ppm from the SPS sample. There are no NMR peaks outside the displayed spectral region, except for two very weak spinning sidebands in the case of the SPS sample. The asterisk marks a small rotor/probehead background signal (verified through the recording of a spectrum from an empty rotor).

The absorption coefficient k was for all samples equal to zero. Overall, apart from the need to assume a very thin C layer (1.80 nm), the refractive index and its dispersion in the visible of the SPS sample are very similar to that of the reference sample, which again proves the structural similarity of both samples.

The enhanced content of OH groups in the SPS-prepared specimen is evidenced further by the ^{1}H MAS NMR spectra displayed in Fig. 7, whose main distinction is the increased signal intensity at 2.9 ppm from the SPS sample. Additionally, a very weak line ~1.2 ppm appears to be present in both spectra, although it is only clearly discernable in that of the reference SiO_2 glass. Signals in the ^{1}H chemical shift region between 1 and 2 ppm usually reflect "isolated" OH groups (i.e., those not experiencing hydrogen bonding), whereas weakly and strongly hydrogen-bonded silanols give NMR signals in the approximate ranges of 3–4 and >5 ppm, respectively [28,29]. Therefore we assign the minor signal ~1.2 ppm to isolated SiOH groups and the main peak ~2.9 ppm to weakly hydrogen-bonded silanols. Adsorbed water is usually the main contributions to signals appearing between 4 and 5 ppm, as usually found in ^{1}H MAS NMR spectra from mesoporous silica-based materials. The absence of a significant intensity in this spectral region (see Fig. 7) suggests that the amounts of physisorbed water molecules must overall be relatively low in both samples and that most protons are present as SiOH groups. The absence of the dynamics associated with mobile water molecules may also explain the relatively long ^{1}H T_1 relaxation times (which are minutes rather than seconds) encountered in both samples.

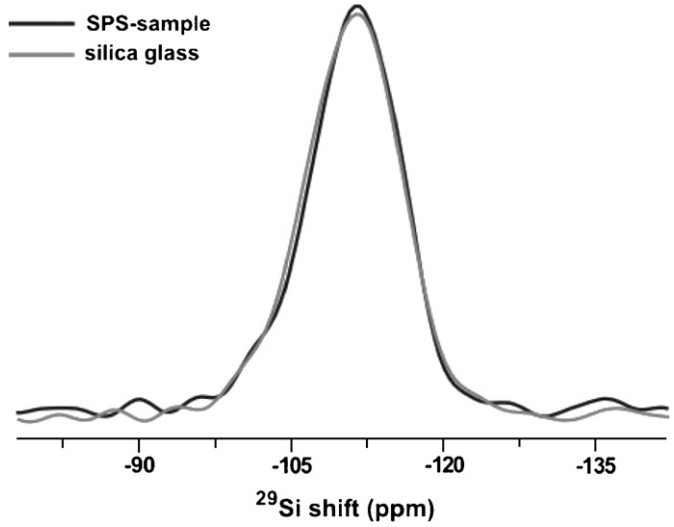

Fig. 8. ^{29}Si MAS NMR spectra recorded from the SPS-prepared (black) and reference sample (gray) of SiO_2.

By comparing peak integrals, we obtained a 6.5-fold higher ^{1}H content in the SPS sample relative to the reference silica glass. This estimate included a correction for the minor saturation of the ^{1}H signals from the reference sample, stemming from the experimentally used relaxation delays of 420 s. Whereas the ^{1}H NMR results give unambiguous proof for a significantly higher H content of the SPS-prepared sample relative to the conventionally prepared silica glass, we note that NMR appears to underestimate the difference between the samples compared to that obtained from IR. We have currently no obvious explanation for this discrepancy.

Fig. 8 displays the corresponding ^{29}Si NMR spectra of the two samples. They are essentially identical within the experimental signal-to-noise ratio and the uncertainties in the chemical shift referencing (±0.15 ppm). Each of the main peaks fitted well to a single Gaussian line of FWHM 11 ppm and centered at −111.4 ppm (SPS sample) and −111.1 ppm (reference). These [29] ^{29}Si NMR peak centers and widths are representative of amorphous SiO_2 samples [30] and evidence that the distributions of Si–O–Si bond angles and inter-atomic distances must, on the average, be very similar in both silica structures.

The results of the thermogravimetric analysis are displayed in Fig. 9. This analysis shows that upon heat treatment, the SPS sample lost about 0.72% in weight between 200 and 360 °C and another 0.22% between 600 and 660 °C. We attribute the first weight loss primarily to dehydration of physisorbed water, whereas the second weight loss is primarily stemming from dehydoxylation processes, according to $2{\equiv}Si{-}OH \rightarrow {\equiv}Si{-}O{-}Si{\equiv}+H_2O$ [31].

4. Conclusion

We have proven the feasibility to use SPS as a method to prepare glassy and transparent materials using SiO_2 as an example. With respect to both, local structural features as well as the overall network hierarchy, the SPS-compacted SiO_2 sample was found to be very similar to conventionally prepared silica glass. The main difference is the enhanced content of OH groups in the SPS-prepared sample, possibly accompanied with minute contaminations of amorphous carbon. We are optimistic that both problems can be solved by process optimization, e.g., by adding an annealing stage prior to densification to remove the water, by

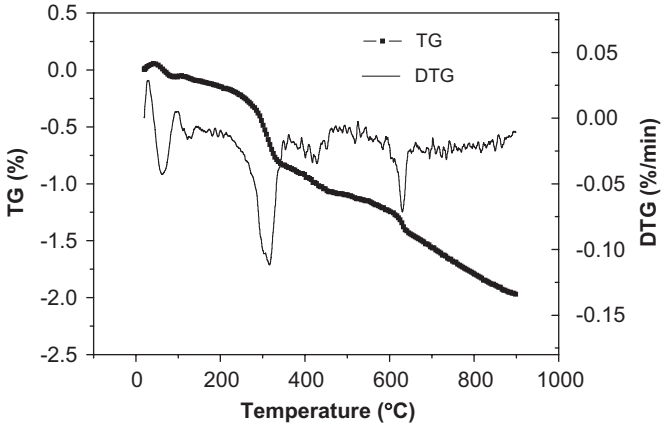

Fig. 9. Weight loss (Δw) and $d(\Delta w)/dt$ plotted versus temperature.

adjusting pressure and temperature of the SPS process or by a fine-tuning of the heat treatment following the SPS process.

The new way of preparing non-metallic glasses as demonstrated in this work is particularly interesting for compositions that are inaccessible by conventional glass manufacturing methods. Therefore, the SPS process may open the way for the preparation of novel classes of glassy materials.

Acknowledgments

Z.S. and M.E. acknowledge funding from the Swedish Research Council (VR) and the Carl Trygger Foundation. We thank Juanfang Ruan for recording the TEM images and Professor Mats Nygren for thermogravimetric analysis as well as for his valuable comments.

References

[1] Z.A. Munir, U. Anselmi-Tamburini, M. Ohyanagi, J. Mater. Sci. 41 (2006) 763.
[2] L. Gao, Z. Shen, H. Miyamoto, M. Nygren, J. Am. Ceram. Soc. 82 (1999) 1061.
[3] M. Nygren, Z.J. Shen, Solid State Sci. 5 (2003) 125.
[4] T.G. Mayerhöfer, Z. Shen, R. Keding, T. Höche, Optik 114 (2003) 351.
[5] Y. Gu, K.A. Khor, P. Cheang, Biomaterials 25 (2004) 4127.
[6] A. Nakahira, M. Tamai, H. Aritatani, S. Nakamura, K. Yamashita, J. Biomed. Mater. Res. 62 (2002) 550.
[7] J.W. Lee, Z.A. Munir, M. Ohyanagi, Mater. Sci. Eng. A 325 (2002) 221.
[8] X.Y. Zhang, S.H. Tan, D.L. Jiang, Ceram. Int. 31 (2005) 267.
[9] C. Shen, Q.F. Liu, Q. Liu, Mater. Lett. 58 (2004) 2302.
[10] Y. Guo, K. Kakimoto, H. Ohsato, Jpn. J. Appl. Phys. 42 (2003) 7410.
[11] S.Y. Lee, S.I. Yoo, Y.W. Kim, N.M. Heang, Y.D. Kim, J. Am. Ceram. Soc. 86 (2003) 1800.
[12] X. Li, A. Chiba, M. Sato, S. Takashash, J. Alloys Compd. 336 (2002) 232.
[13] R. Chaim, Z. Shen, M. Nygren, J. Mater. Res. 19 (2004) 2527.
[14] Z.Y. Fu, J.F. Liu, H. Wang, D.H. He, Q.J. Zhang, Mater. Sci. Technol. 20 (2004) 1097.
[15] C.K. Kim, H.S. Lee, S.Y. Shin, J.C. Lee, D.H. Kim, S. Lee, Mater. Sci. Eng. A 406 (2005) 293.
[16] M.S. El-Eskandarany, A. Omori, A. Inoue, J. Mater. Res. 20 (2005) 2845.
[17] T.S. Kim, J.K. Lee, H.J. Kim, J.C. Bae, Mater. Sci. Eng. A 402 (2005) 228.
[18] W. Vogel, Glass Chemistry, Springer, Berlin, 1994.
[19] F.L. Galeener, A.J. Leadbetter, M.W. Stringfellow, Phys. Rev. B 27 (1983) 1052.
[20] T.G. Mayerhöfer, H.H. Dunken, R. Keding, C. Rüssel, J. Non-Cryst. Solids 333 (2004) 172.
[21] C.T. Kirk, Phys. Rev. B 38 (1988) 1255.
[22] P.G. Pai, S.S. Chao, Y. Takagi, G. Lucovsky, J. Vac. Sci. Technol. A 4 (1986) 689.
[23] G. Lucovsky, C.K. Wong, W.B. Pollard, J. Non-Cryst. Solids 59+60 (1983) 839.
[24] E.I. Kamitsos, A.P. Patsis, G. Kordas, Phys. Rev. B 48 (1993) 12499.
[25] R.H. Stolen, G.E. Walrafen, J. Chem. Phys. 64 (1976) 2623.
[26] J.B. Bates, R.W. Hendriks, L.B. Shaffer, J. Chem. Phys. 61 (1974) 4163.
[27] The presence of carbon could not be proved by Raman spectroscopy.
[28] I.S. Chuang, D.R. Kinney, G.E. Maciel, J. Am. Chem. Soc 115 (1993) 8695.
[29] C.C. Liu, G.E. Maciel, J. Am. Chem. Soc 118 (1996) 5103.
[30] K.J.D. McKenzie, M.E. Smith, Multinuclear Solid-State NMR of Inorganic Materials, Pergamon Press, Amsterdam, 2002.
[31] Yu.D. Glinka, M. Jaroniec, J. Appl. Phys. 82 (1997) 3499.